



**HAL**  
open science

## The exon-junction-complex-component metastatic lymph node 51 functions in stress-granule assembly.

Aurélie Baguet, Sébastien Degot, Nicolas Cougot, Edouard Bertrand, Marie-Pierre Chenard, Corinne Wendling, Pascal Kessler, Hervé Le Hir, Marie-Christine Rio, Catherine Tomasetto

### ► To cite this version:

Aurélie Baguet, Sébastien Degot, Nicolas Cougot, Edouard Bertrand, Marie-Pierre Chenard, et al.. The exon-junction-complex-component metastatic lymph node 51 functions in stress-granule assembly.. *Journal of Cell Science*, 2007, 120 (Pt 16), pp.2774-84. 10.1242/jcs.009225 . hal-00189164

**HAL Id: hal-00189164**

**<https://hal.science/hal-00189164v1>**

Submitted on 1 Jun 2021

**HAL** is a multi-disciplinary open access archive for the deposit and dissemination of scientific research documents, whether they are published or not. The documents may come from teaching and research institutions in France or abroad, or from public or private research centers.

L'archive ouverte pluridisciplinaire **HAL**, est destinée au dépôt et à la diffusion de documents scientifiques de niveau recherche, publiés ou non, émanant des établissements d'enseignement et de recherche français ou étrangers, des laboratoires publics ou privés.

# The exon-junction-complex-component metastatic lymph node 51 functions in stress-granule assembly

Aurélie Baguet<sup>1</sup>, Sébastien Degot<sup>1,\*</sup>, Nicolas Cougot<sup>2</sup>, Edouard Bertrand<sup>2</sup>, Marie-Pierre Chenard<sup>3</sup>, Corinne Wendling<sup>1</sup>, Pascal Kessler<sup>1</sup>, Hervé Le Hir<sup>4</sup>, Marie-Christine Rio<sup>1</sup> and Catherine Tomasetto<sup>1,‡</sup>

<sup>1</sup>Institut de Génétique et de Biologie Moléculaire et Cellulaire (IGBMC), Département de Biologie du Cancer, UMR 7104 CNRS/ U596 INSERM/ Université Louis Pasteur, BP 10142, 67404 Illkirch, C.U. de Strasbourg, France

<sup>2</sup>Institut de Génétique Moléculaire de Montpellier, CNRS UMR 5535- IFR 24, 1919 route de Mende 34000 Montpellier, France

<sup>3</sup>Département de Pathologie Générale, Centre Hospitalier Universitaire de Haute-pierre, 67098 Strasbourg, France

<sup>4</sup>Centre de Génétique Moléculaire, CNRS UPR2167, Avenue de la Terrasse, 91198 Gif-sur-Yvette, France

\*Present address: Department of Biological Chemistry and Molecular Pharmacology, Harvard Medical School, Boston, MA 02115, USA

‡Author for correspondence (e-mail: cat@igbmc.u-strasbg.fr)

Accepted 11 June 2007

Journal of Cell Science 120, 2774-2784 Published by The Company of Biologists 2007

doi:10.1242/jcs.009225

## Summary

Metastatic lymph node 51 [MLN51 (also known as CASC3)] is a component of the exon junction complex (EJC), which is assembled on spliced mRNAs and plays important roles in post-splicing events. The four proteins of the EJC core, MLN51, MAGOH, Y14 and EIF4AIII shuttle between the cytoplasm and the nucleus. However, unlike the last three, MLN51 is mainly detected in the cytoplasm, suggesting that it plays an additional function in this compartment. In the present study, we show that MLN51 is recruited into cytoplasmic aggregates known as stress granules (SGs) together with the SG-resident proteins, fragile X mental retardation protein (FMRP), poly(A) binding protein (PABP) and poly(A)<sup>+</sup> RNA. MLN51 specifically associates with SGs via its C-terminal

region, which is dispensable for its incorporation in the EJC. MLN51 does not promote SG formation but its silencing, or the overexpression of a mutant lacking its C-terminal region, alters SG assembly. Finally, in human breast carcinomas, MLN51 is sometimes present in cytoplasmic foci also positive for FMRP and PABP, suggesting that SGs formation occurs in malignant tumours.

Supplementary material available online at

<http://jcs.biologists.org/cgi/content/full/120/16/2774/DC1>

Key words: Stress granule, MLN51, Barentsz, FMRP, DCP1, Breast cancer

## Introduction

Human metastatic lymph node 51 (MLN51; also known as CASC3) was identified as a gene overexpressed in malignant breast tumours (Tomasetto et al., 1995). MLN51 is a nucleocytoplasmic protein containing, within its amino-terminal half, a coiled-coil domain followed by two nuclear localization signals (NLSs) responsible for nuclear localization and, in its carboxyl-terminal half, a nuclear export signal (NES) that mediates cytoplasmic retention (Degot et al., 2002; Macchi et al., 2003). Interestingly, MLN51 contains a conserved region named SELOR for speckle localizer and RNA binding module, which binds RNA directly, interacts with MAGOH and/or Y14 (also known as RBM8A) and spliced mRNA, and addresses the protein to subnuclear regions called nuclear speckles (Degot et al., 2004) where most of the EJC factors are localized (Custodio et al., 2004). MLN51 is a mRNA-binding protein in mammalian cells (Degot et al., 2004), and in the fly, a trans-acting factor involved in *oskar* mRNA localization (van Eeden et al., 2001). Like the other trans-acting factors involved in *oskar* mRNA localization [mago nashi (human homologue, MAGOH), tsunagi (Y14) and EIF4AIII (EIF4AIII)] MLN51 is a component of the exon junction complex (EJC) in mammalian cells (Degot et al., 2004; Tange et al., 2005).

The multi-protein EJC is assembled onto nascent mRNA in a sequence-independent manner at a defined position located

20-24 nucleotides upstream of the exon-exon junction (Le Hir et al., 2000; Tange et al., 2004). To date, the EJC is known to be composed of at least eleven proteins: MAGOH, Y14, RNPS1, SRm160, REF, UAP56, EIF4AIII, MLN51, SAP18, Acinus and Pinin (Tange et al., 2005). EJC composition is dynamic; several EJC factors function both in the nucleus and in the cytoplasm whereas others simply function in the nucleus and/or during mRNA nuclear export (Tange et al., 2004). Accordingly, the EJC core is formed by the stable association of a few proteins with newly spliced mRNA, which provides an anchoring point for other factors involved in distinct mRNA functions such as mRNA transport, nonsense-mediated mRNA decay and translation (Palacios et al., 2004; Nott et al., 2004; Tange et al., 2005; Gehring et al., 2005). In vitro, the recombinant proteins: MLN51, MAGOH, Y14 and EIF4AIII are necessary and sufficient to form a stable complex on single-stranded RNA in the presence of ATP (Ballut et al., 2005). A similar finding was shown using co-immunoprecipitation of mRNA spliced in vitro (Tange et al., 2005). Thus, the tetrameric association of MLN51, MAGOH, Y14 and EIF4AIII with RNA represents the minimal EJC core (Ballut et al., 2005; Tange et al., 2005). The SELOR domain of MLN51 is sufficient to form the stable EJC core complex and mutations at conserved residues within this region prevent complex assembly in vitro and in vivo (Ballut et al., 2005). Recently, the structure of the core complex was solved in the

presence of an ATP analogue and a polyuracil mRNA mimic (Andersen et al., 2006; Bono et al., 2006). Within the complex, EIF4AIII binds RNA with the phosphate sugar backbone of six consecutive nucleotides. The SELOR domain of MLN51 also binds RNA directly with one nucleotide and increases RNA binding efficiency when bound to EIF4AIII. The MAGOH and Y14 subunits are probably involved into the regulation of ATPase hydrolysis inside the tetrameric complex (Andersen et al., 2006; Bono et al., 2006).

Each component of the EJC core shuttles between the nucleus and the cytoplasm. At steady state, EIF4AIII, MAGOH and Y14 are mainly localized in the nucleus (Kataoka et al., 2000; Le Hir et al., 2001; Palacios et al., 2004; Shibuya et al., 2004) whereas MLN51 is predominantly in the cytoplasm (Degot et al., 2002). This cytoplasmic localization of MLN51 suggests that MLN51 might also function in the cytoplasm. In the work described here we studied the localization of MLN51 under conditions where mRNA metabolism is altered. During stress, MLN51 is recruited to mRNA storage regions known as stress granules (SGs). These regions store untranslated mRNAs and contain a variety of mRNA binding proteins (Anderson and Kedersha, 2006). We show that MLN51 localization in SGs is mediated by its C-terminal region and that loss of MLN51 alters SG formation. Finally, we show that, in human breast cancer biopsies, cancer cells sometimes accumulate MLN51 in discrete cytoplasmic foci resembling SGs.

## Results

### MLN51 is recruited to SGs

MLN51 is found in distinct cellular locations when it is overexpressed in cultured cells. EYFP-tagged MLN51 proteins were found to be diffuse in the cytoplasm (supplementary material Fig. S1Aa), in small cytoplasmic foci (supplementary material Fig. S1Ab) or in larger cytoplasmic foci (supplementary material Fig. S1Ac). These foci are reminiscent of decapping enzyme-containing (Dcp) bodies and SGs. Dcp bodies (also known as P-bodies) contain mRNAs destined for degradation (Cougot et al., 2004; Eulalio et al., 2007; Parker and Sheth, 2007) or storage of repressed mRNA (Pillai et al., 2005; Liu et al., 2005) whereas SGs contain stored mRNAs whose translation was stopped in response to stress (Anderson and Kedersha, 2006). To test whether endogenous MLN51 is recruited to SGs under stress, we studied its subcellular localization after arsenite treatment of HeLa cells. In the absence of arsenite, endogenous MLN51 was mainly detected in the cytoplasm with a faint staining in the nucleus (Fig. 1Aa-c). In the presence of arsenite (500  $\mu$ M for 1 hour), MLN51 was detected in cytoplasmic granules positive for FMRP (also known as FMR1; Fig. 1Ad-f). The recovery patterns of both MLN51 and FMRP were monitored after arsenite wash-out and incubation in normal medium. After a 1-hour recovery, most of the MLN51 and FMRP proteins were still in the SGs, which continued to increase in size but decrease in number. In these cells, the signals appeared more diffuse than under stress conditions (compare Fig. 1Ag-i with 1Ad-f). After 2 hours recovery, in most cells, both MLN51 and FMRP were no longer in foci and had returned to their normal localization throughout the cytoplasm (Fig. 1Aj-l). A similar recovery pattern was previously described for the SG-resident protein TIA1 (Kedersha and Anderson, 2002). To verify that during stress, MLN51 is an exclusive component of SGs, we

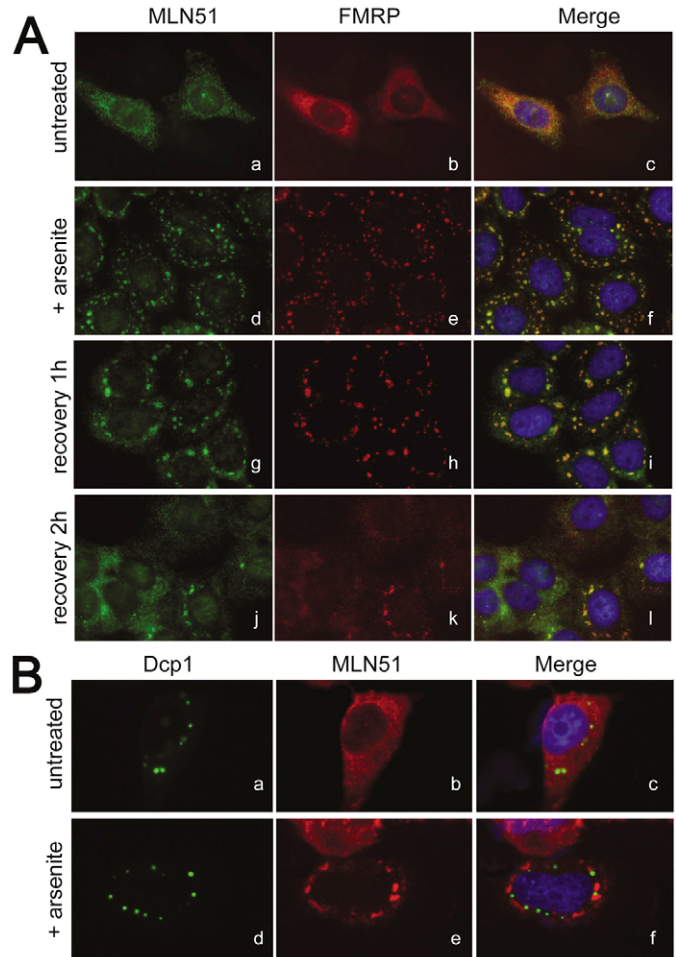


**Fig. 1.** The endogenous MLN51 protein is recruited to SGs.

(A) Immunofluorescence analysis of MLN51 and FMRP mobilization into SGs after arsenite treatment. HeLa cells, control (a-c, untreated) or treated with 0.5 mM arsenite for 1 hour (d-f) were either immediately fixed (a-f) or allowed to recover for 1 (g-i) or 2 (j-l) hours in normal medium without arsenite prior to fixation. Next, cells were co-labelled with anti-MLN51 (a,d,g,j, green) and anti-FMRP (b,e,h,k, red) antibodies. Nuclei were counterstained with Hoechst 33258 (blue) and corresponding merged images are shown on the right (c,f,i,l). (B) Immunofluorescence analysis of HeLa cells transiently transfected with the pEGFP-DCP1 plasmid (green). Control- and arsenite-treated cells were stained with an anti-MLN51 antibody (red), nuclei were counterstained with Hoechst 33258 (blue). Note that the endogenous MLN51 protein is not recruited into Dcp bodies.

performed colocalization studies for MLN51 and GFP-DCP1A. No colocalization was apparent either under normal or stress conditions (Fig. 1B). To confirm that MLN51 is a normal component of SGs, we treated cells with thapsigargin, a stress-inducer that induces the unfolded protein response, a cellular response to the accumulation of misfolded proteins in the endoplasmic reticulum (Marciniak et al., 2006; Zhang and Kaufman, 2006). Following thapsigargin treatment, MLN51 was also recruited to SGs (data not shown).

Under normal conditions, both MLN51 and FMRP

are present in the cytoplasm where they do not co-localize. Under stress conditions, MLN51 is present in SGs containing both TIA1 and FMRP (Fig. 2A). To better visualize SG architecture, we used high-resolution confocal imaging of arsenite-treated HeLa cells co-labelled with anti-FMRP and anti-MLN51 antibodies (Fig. 2B). On average, all SGs appeared positive for both proteins (Fig. 2B). However, high magnification of a SG section showed that it is composed of a mixture of microdomains enriched in FMRP, MLN51 or both proteins (Fig. 2B, inserts).

We next tested if MLN51 shuttles in and out of SGs. We performed fluorescence recovery after photobleaching (FRAP) analysis on EYFP- or GFP-tagged proteins. Cells were transfected with EYFP-MLN51 full length, C-terminal fragment (EYFP-MLN51Ct), GFP-hnRNPA1 or GFP-PABP. They were treated with arsenite 48 hours after transfection, and subjected to FRAP. Results indicate that MLN51 and

MLN51Ct are rapidly exchanged from SGs ( $t_{1/2}$  of 21 seconds and 12 seconds, respectively), and only a small fraction were immobile (19% for MLN51 full length and 9% for EYFP-MLN51Ct; Fig. 2Ca-c). Interestingly MLN51Ct moved in and out of SGs very rapidly, like hnRNPA1 (Fig. 2C) (Guil et al., 2006) and TIA1 (Guil et al., 2006; Kedersha et al., 2000). By contrast, as previously described, PABP exhibited much slower movement and a poor recovery, probably reflecting the slow movement of mRNAs (Fig. 2C) (Guil et al., 2006).

#### Recruitment of MLN51 to SGs does not require its association with the exon junction complex

To evaluate which region of MLN51 is involved in its recruitment to SGs, several deletion mutants (Fig. 3A) were expressed in HeLa cells under arsenite-stress conditions. The full-length protein, EYFP-MLN51/1-703 and the C-terminal half fragment (EYFP-MLN51/377-703) were present in SGs, as traced with FMRP (Fig. 3Ba,c). By contrast, the N-terminal-half fragment (EYFP-MLN51/1-383), containing the SELOR module and the NLSs, was not present in SGs but showed a diffuse nucleocytoplasmic localization (Fig. 3Bb). Finally, a mutant devoid of the N-terminal and C-terminal extremities of the protein (EYFP-MLN51/277-481) was not detected in SGs (Fig. 3Bd). We next tested the potential recruitment of two EJC proteins, MAGO and Y14, to SGs. Under stress, EYFP-tagged

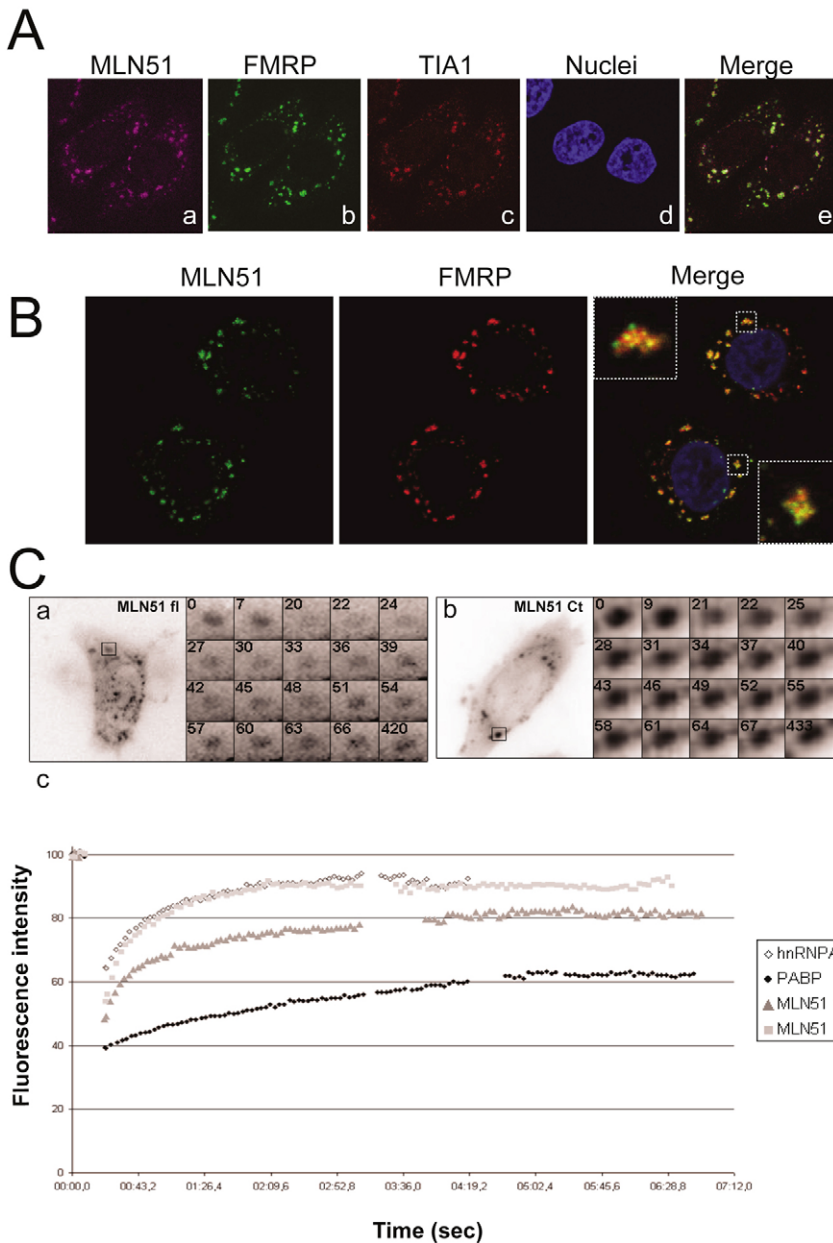


**Fig. 2.** SGs show discrete microdomains and dynamic shuttling of some components. (A) SGs are positive for MLN51, TIA1 and FMRP.

Arsenite-treated HeLa cells, were fixed and co-labelled with anti-MLN51 (a, purple), anti-TIA1 (c, red) and anti-FMRP (b, green) antibodies. Nuclei were counterstained with Hoechst (d, blue) and the merged image of a, b and c is shown in e. (B) Confocal analysis of MLN51 and FMRP distribution into SGs. Arsenite-treated cells were co-labelled using anti-MLN51 (green) and anti-FMRP (red) antibodies and with Hoechst (blue). One section of 200 nm of the merge image is shown; inserts on the top left and lower right inside are higher magnification (2.5 fold) images of the SGs present in dotted squares. (C) FRAP analysis of MLN51FL and MLN51Ct mobilization into SGs after arsenite treatment. HeLa cells transfected with EYFP-tagged MLN51 full length (fl) and MLN51/377-703 (Ct) and GFP-tagged hnRNPA1 and PABP for 48 hours and treated with arsenite were analysed by FRAP. One representative cell expressing EYFP-MLN51FL (a) or EYFP-MLN51Ct (b) is shown. In both cases one granule (square boxes) was bleached and pictures were taken every 3 seconds. Time is indicated in seconds on each picture. (c) Graphical representation of fluorescence recovery patterns. Curves represent fluorescence intensity over time (seconds) and each curve corresponds to ten independent experiments.

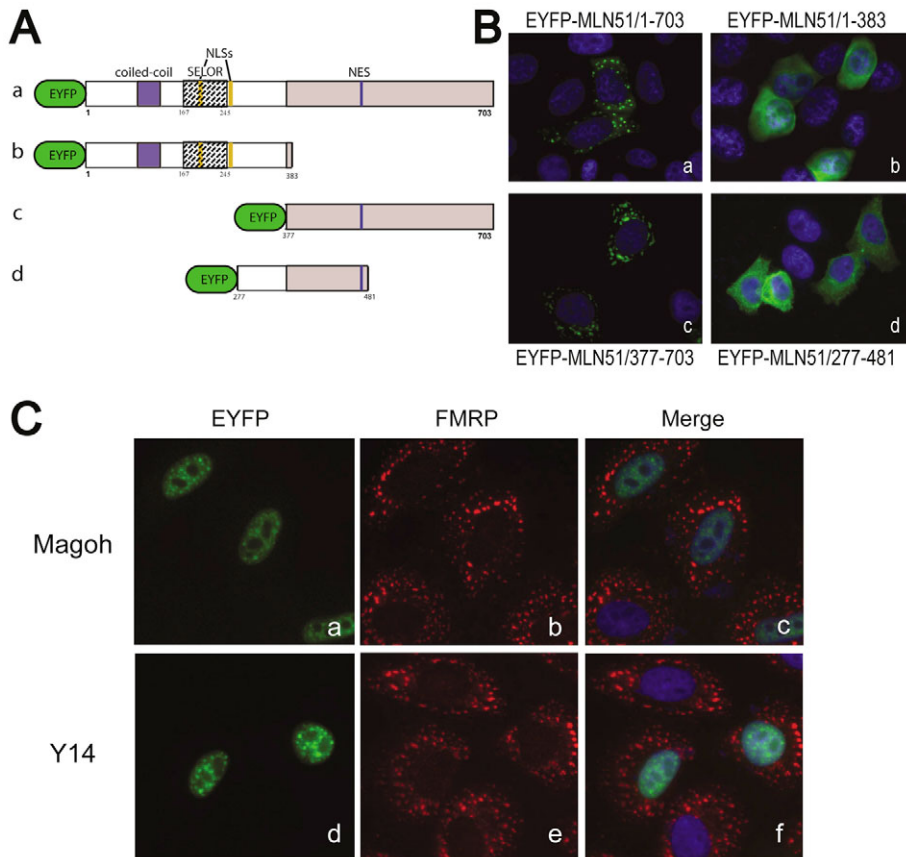


**Fig. 3.** Recruitment of MLN51 to SGs does not require its association with the exon junction complex. (A) Schematic representation of MLN51-derived constructs, indicating different consensus motifs including the SELOR module. The white and grey boxes show the position of the N- and C-terminal constructs, respectively. (B) Immunofluorescence analysis of HeLa cells transfected with full length and truncated EYFP-tagged MLN51 proteins (green). Arsenite-treated cells were fixed 24 hours, after transfection. (C) Immunofluorescence analysis of HeLa cells transfected with EYFP-tagged MAGOH (a,c, green) and Y14 (d,f, green). Arsenite-treated cells were stained with an anti-FMRP antibody (b,e, red). Nuclei were counterstained with Hoechst (blue).

MAGOH and Y14 were mainly detected in the nucleus in ring-shape structures typical of nuclear speckles (Fig. 3Ca,d) and were absent from cytoplasmic SGs as traced with FMRP (Fig. 3Cb,e). Taken together, these results show that MLN51 is recruited into SGs via its C-terminal domain, independent of its association with the EJC. In agreement with this, under stress conditions, MAGOH and Y14 were also absent from SGs.

#### Overexpression of MLN51 does not induce SG formation

It was shown that SG assembly can be induced in non-stressed cells by overexpressing a variety of proteins including a phosphomimetic mutant of the translation initiation factor EIF2 $\alpha$ , the Ras-GAP-SH3-binding protein (G3BP), FMRP and the cytoplasmic polyadenylation element-binding protein 1 (CPEB1) (Kedersha et al., 1999; Tourriere et al., 2003; Mazroui et al., 2002; Wilczynska et al., 2005). As shown in supplementary material Fig. S1Ab,c, transient transfection of EYFP-MLN51 correlates occasionally with the presence of

SGs in transfected cells. This localization is probably due to cellular stress inherent to the transient transfection procedure (supplementary material Fig. S1C). Nevertheless, to clarify the role of MLN51 in SG formation, we used an overexpression system which does not require transient transfection, in which MLN51 overexpression is driven by an inducible promoter in HeLa cells (Gossen et al., 1995).

HeLa Tet-On cells were stably transfected with plasmids allowing the inducible expression of the complete protein pUHD-MLN51/1-703 (MLN51Fl), the N-terminal part pUHD-MLN51/1-383 (MLN51Nt) or with the empty vector pUHD (control). Clones showing a significant upregulation of MLN51Fl or MLN51Nt in the presence of doxycyclin were selected for further study (Fig. 4A). HeLa Tet-On MLN51Fl cells, treated with doxycyclin, did not show the presence of SGs, traced here with FMRP and poly(A)<sup>+</sup> RNAs (Fig. 5Aa-f). Similarly, overexpression of MLN51Nt did not induce SG formation (Fig. 5Am-r). To verify that SG assembly was not altered by MLN51 overexpression, both cell lines were treated with arsenite after doxycyclin induction (Fig. 5Ag-l,s-x). MLN51 overexpression did not modify SGs traced here by the accumulation of MLN51, FMRP and poly(A)<sup>+</sup> RNAs (Fig. 5Ag-l). Surprisingly, overexpression of MLN51Nt prevented SG assembly, as shown by the absence of cytoplasmic foci containing FMRP and poly(A)<sup>+</sup> RNAs (Fig. 5As-x).

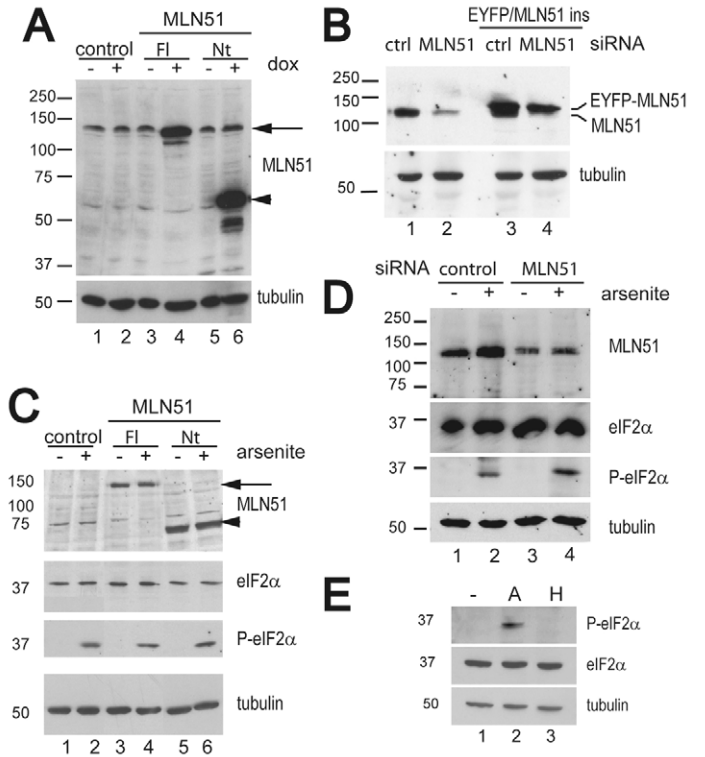
#### MLN51 acts independently of EIF2 $\alpha$ phosphorylation during SG formation

To further explore the potential role of MLN51 during SG formation, we tested whether transient overexpression of MLN51Nt would also alter SG formation. HeLa cells were transiently transfected with Flag- or EYFP-tagged MLN51Nt constructs. Cells were treated with arsenite 24 hours after transfection. Cells showing a high level of MLN51Nt protein lacked FMRP-positive SGs (Fig. 5Ba-c,d-f). Cells expressing high levels of MLN51Fl had normal FMRP-positive SGs. These results suggest that the MLN51Nt protein, lacking the C-terminal region, might function as a dominant-negative for the formation of SGs.

To confirm this hypothesis we tested whether reducing MLN51 protein levels by siRNA in HeLa cells would also prevent SG formation. Western blot analysis of total cellular extracts revealed that a 50-70% reduction in MLN51 levels can be obtained by siRNA transfection (Fig. 4B, lanes 1 and 2). Three days after transfection, HeLa cells were treated with

**Fig. 4.** Up- and downregulation of MLN51 in HeLa cells.

(A) Western blot containing ~20  $\mu$ g of total protein obtained from: HeLa Tet-On control cells (lanes 1 and 2) stably transfected with the empty pUHD vector; HeLa Tet-On MLN51Fl (lanes 3 and 4) and HeLa Tet-On MLN51Nt (lanes 5 and 6) cells, transfected with pUHD-MLN51/1-703 and pUHD-MLN51/1-383, respectively. The blot was probed with an anti-MLN51 against the SELOR domain of MLN51 and then probed with an anti-tubulin antibody which was used as a loading control. A 24-hour induction with doxycyclin is indicated on the top (+dox). The Arrow and arrowhead on the right indicate the position of MLN51Fl and MLN51Nt, respectively. (B) Western blot analysis of MLN51 depletion in HeLa cells. Western blot containing 20  $\mu$ g of total protein obtained from HeLa cells transfected twice with either synthetic control siRNA (lanes 1 and 3) or MLN51-specific siRNA (lanes 2 and 4), and with pEYFP-MLN51ins plasmid was probed with anti-MLN51 and anti-tubulin (loading control) antibodies. The positions of the endogenous MLN51 and of the EYFP-MLN51 fusion protein are indicated on the right. (C) Analysis of arsenite-induced EIF2 $\alpha$  (eIF2 $\alpha$ ) phosphorylation in the presence of MLN51Fl and MLN51Nt. 20  $\mu$ g of total protein obtained from doxycyclin-induced HeLa Tet-On control (lanes 1 and 2); HeLa Tet-On MLN51Fl (lanes 3 and 4) and HeLa Tet-On MLN51Nt (lanes 5 and 6) cells, treated (+) or not (-) with arsenite, were analysed by western blotting using anti-MLN51-, anti-EIF2 $\alpha$ -, anti-phospho-EIF2 $\alpha$ - and anti-tubulin-specific antibodies. Arrow and arrowhead on the right indicate the position of MLN51Fl and MLN51Nt, respectively. (D) Analysis of arsenite-induced EIF2 $\alpha$  phosphorylation in MLN51-silenced cells. 20  $\mu$ g of total protein obtained from HeLa cells transfected twice with either synthetic control siRNA (lanes 1 and 2) or MLN51-specific siRNA (lanes 3 and 4), treated (+) or not (-) with arsenite, were analysed by western blotting using anti-MLN51-, anti-EIF2 $\alpha$ -, anti-phospho-EIF2 $\alpha$ - and anti-tubulin-specific antibodies. (E) Analysis of EIF2 $\alpha$  phosphorylation in HeLa cells treated with arsenite or hippuristanol. 20  $\mu$ g of total protein obtained from HeLa cells untreated (-, lane 1), treated with arsenite (A, lane 2) or with hippuristanol (H, lane 3) were analysed by western blotting using anti-EIF2 $\alpha$ -, anti-phospho-EIF2 $\alpha$ - and anti-tubulin-specific antibodies.



arsenite and analyzed for MLN51 silencing and SG formation via MLN51 and FMRP immunostaining, respectively. Treatment of cells with MLN51 siRNA significantly altered SG formation (Fig. 6A, upper panel). The response to siRNA MLN51 transfection was not complete and residual SGs were occasionally seen in some cells. From two independent experiments performed in triplicate, we found that the reduction of MLN51 by siRNA significantly reduced the number of cells forming SGs under arsenite treatment (Fig. 6B;  $P < 0.001$ ). To test whether MLN51 expression could rescue SG formation in silenced cells, a siRNA-insensitive EYFP-MLN51 mutant plasmid (pEYFP-MLN51ins) was introduced into siRNA-MLN51-transfected HeLa cells. All arsenite-treated cells overexpressing EYFP-MLN51ins contained SGs, as traced with FMRP (Fig. 6A, bottom panel).

To further understand the role of MLN51 on SG assembly, we looked at the effect of MLN51 overexpression on EIF2 $\alpha$  phosphorylation. Inhibition of translation by arsenite treatment induces phosphorylation of EIF2 $\alpha$ , leading to a decrease in the translation initiation rate (Kedersha et al., 2002). HeLa Tet-On MLN51Fl, HeLa Tet-On MLN51Nt and HeLa Tet-On control cells, pre-treated with doxycyclin, were exposed to arsenite. Cellular lysates were analyzed by western blot (Fig. 4C). Using an antibody specific for phosphorylated EIF2 $\alpha$ , we found that EIF2 $\alpha$  phosphorylation was unaffected in cells overexpressing MLN51Fl or MLN51Nt (Fig. 4C, compare lanes 4 and 6 with lane 2). Similarly, MLN51 depletion by siRNA had no effect

on arsenite-induced EIF2 $\alpha$  phosphorylation (Fig. 4D, compare lanes 2 and 4). Recently, the EIF4A inhibitors pateamine A and hippuristanol were found to induce SG formation independently of EIF2 $\alpha$  phosphorylation (Bordeleau et al., 2006; Mazroui et al., 2006). We looked at the effect of MLN51 on SG assembly following hippuristanol treatment. In HeLa cells, hippuristanol triggered SG formation in the absence of EIF2 $\alpha$  phosphorylation (Mazroui et al., 2006) (and Fig. 4E), as shown by the accumulation of FMRP- and MLN51-positive foci (Fig. 5Ca-c). Overexpression of MLN51Fl had no effect on hippuristanol-induced SGs, traced using FMRP (Fig. 5Cd-f). By contrast, overexpression of MLN51Nt impaired their formation (Fig. 5Cg-i), as seen by the diffuse cytoplasmic staining of FMRP, indicating that MLN51 down regulation also inhibits hippuristanol-induced SGs. These results show that loss of MLN51 alters SG assembly in an EIF2 $\alpha$ -independent manner.

Exactly how MLN51 is involved in SG formation is unclear. It was previously reported that SG formation depends on microtubule transport (Ivanov et al., 2003) and on chaperone activity (Gilks et al., 2004). Similarly to Ivanov et al. (Ivanov et al., 2003), we found that in HeLa cells, nocodazole (a microtubule-disrupting agent) treatment prevented arsenite-induced SG assembly (supplementary material Fig. S2). As a link between MLN51 and microtubule-dependent (MT) transport has been established in the fly (van Eeden et al., 2001; Wilhelm et al., 2003), we reasoned that MLN51 might act on

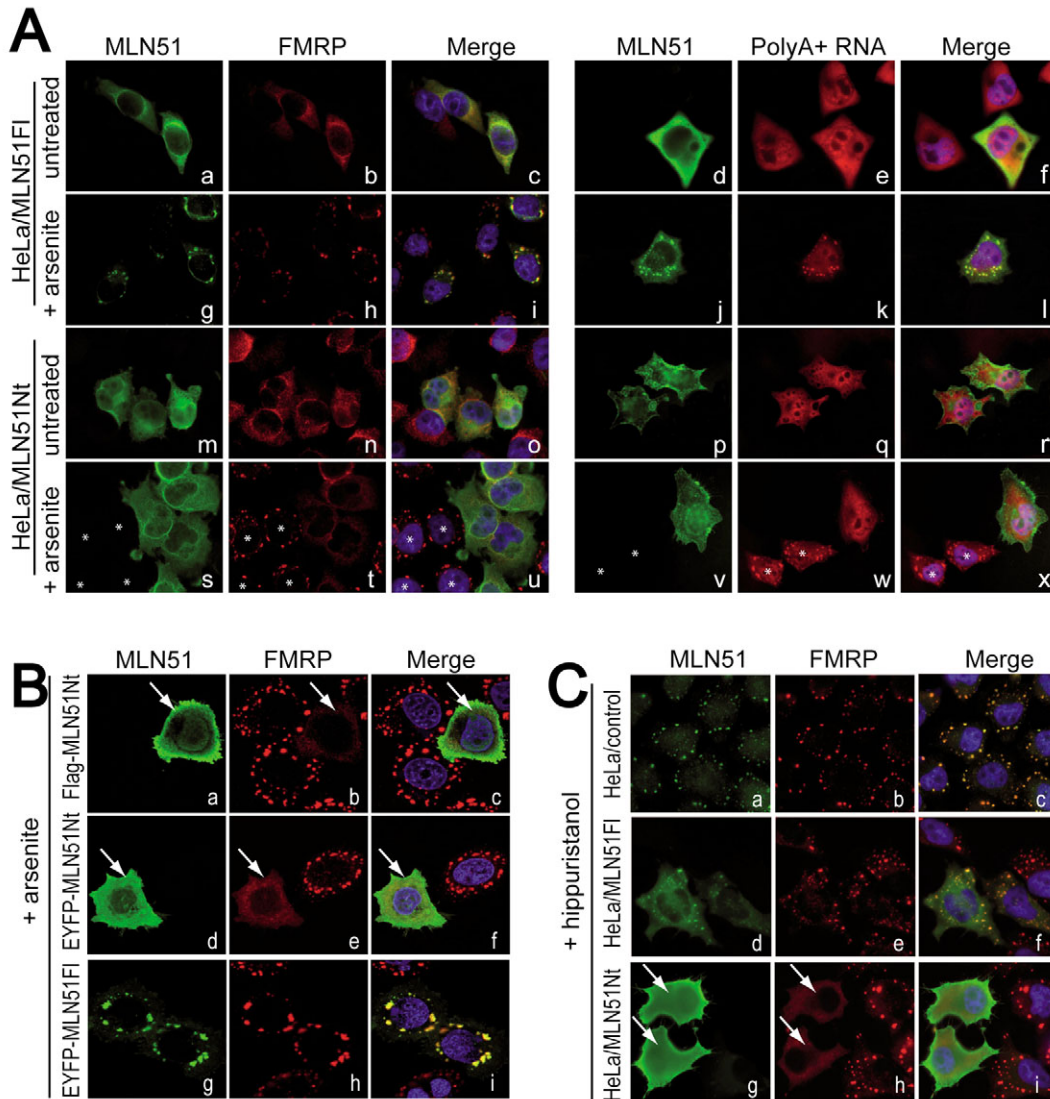
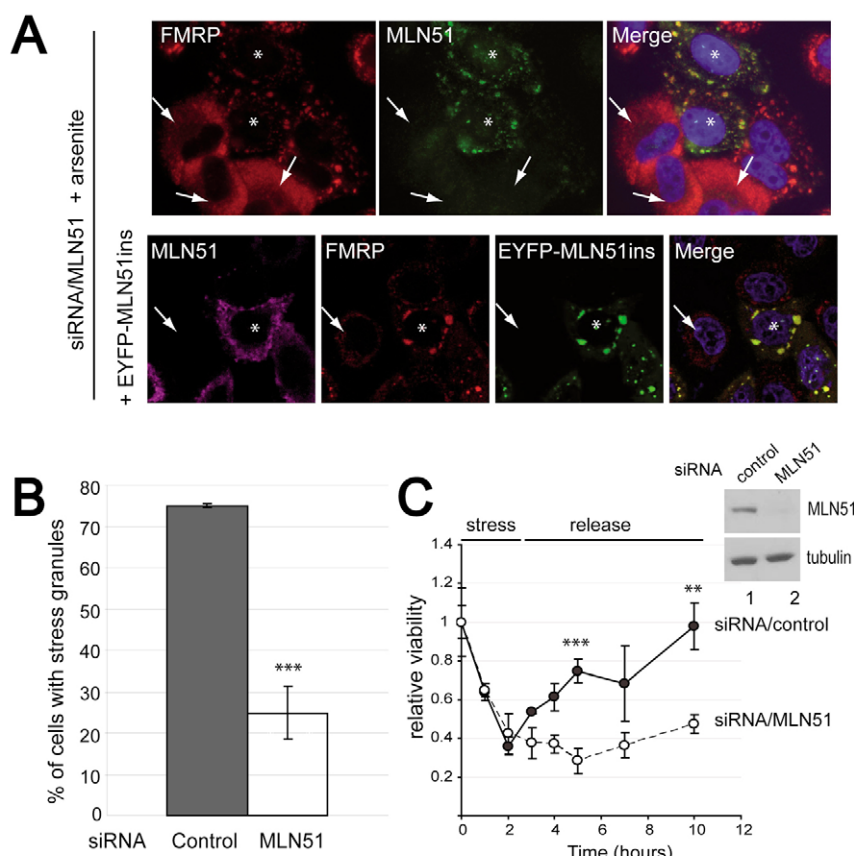


**Fig. 5.** MLN51 downregulation alters SG assembly. (A) HeLa Tet-On MLN51FI (a-l) and HeLa Tet-On MLN51Nt (m-x) were induced for 24 hours with doxycyclin and incubated in normal medium (untreated) or with arsenite for 30 minutes before fixation. Cells were double-stained with anti-MLN51 (green) and anti-FMRP (red) antibodies or with anti-MLN51 (green) antibody and a fluorescent oligo(dT) probe (red) to detect poly(A)<sup>+</sup> RNA as indicated on the top. Note that cells expressing MLN51Nt treated with arsenite do not have FMRP or poly(A)<sup>+</sup> RNA cytoplasmic foci compared with the non-induced cells present in the same fields (asterisks). (B) HeLa cells, transfected with Flag-tagged MLN51Nt (a-c), EYFP-tagged MLN51Nt (d-f, green) and as control EYFP-tagged MLN51FI (g-i, green) plasmids, were treated with arsenite before fixation and probed with anti-Flag (a,c, green) and/or anti-FMRP (red, b,c,e,f,h,i) antibodies. Note that in the merged images (c,f), cells overexpressing Flag-MLN51Nt or EYFP-MLN51Nt have no FMRP-positive cytoplasmic foci (arrows). (C) HeLa control cells (a-c) were treated with hippuristanol before fixation and probed with anti-MLN51 (green, a,c) and anti-FMRP (red, b,c) antibodies. HeLa Tet-On MLN51FI (d-f) and HeLa Tet-On MLN51Nt (g-i) were induced for 24 hours with doxycyclin and incubated with hippuristanol before fixation. Cells were double-stained with anti-MLN51 (green) and anti-FMRP (red) antibodies. Note that cells overexpressing MLN51Nt have no FMRP-positive cytoplasmic foci (arrows).

MT transport of mRNA in SGs. However, in co-labelling and co-immunoprecipitation experiments, we failed to establish a direct link between MLN51 and tubulin or the kinesin heavy chain (not shown). Gilks et al. (Gilks et al., 2004) showed that TIA1 and molecular chaperones (HSP70, HSP27 and HSP40) are key regulators of SG assembly and/or disassembly. We looked at the effect of MLN51Nt overexpression and of MLN51 depletion on chaperone expression. Using western blotting, no induction of HSP70 or HSP40 was observed in stressed cells

overexpressing MLN51Nt and in stressed cells in which MLN51 expression was depleted by siRNA (not shown). Furthermore, pEYFP-MLN51Nt was transfected in HeLa cells, treated with arsenite, sorted using fluorescence-activated cell sorting (FACS), and the HSP70 intracellular signal was measured in EYFP-positive and -negative cells. No significant modification of HSP70 levels was found in cells overexpressing MLN51Nt (not shown). More studies will be necessary to understand the mode of action of MLN51 on SG formation.

**Fig. 6.** Depletion of MLN51 reduces cell viability after stress release. (A) Upper panel: HeLa cells were transfected twice with a MLN51-specific siRNA, treated with arsenite before fixation and double stained with anti-MLN51 (green) and anti-FMRP (red) antibodies. Cells showing undetectable level of MLN51 and no FMRP-positive foci are indicated by arrows and cells showing no depletion of MLN51 and FMRP-positive foci are indicated by asterisks. Bottom panel, MLN51-silenced HeLa cells were transfected using a siRNA-insensitive plasmid pEYFP-MLN51ins and treated with arsenite and stained with anti-MLN51 (purple) and anti-FMRP (red) antibodies. A cell showing undetectable level of MLN51 and no FMRP-positive foci is indicated by an arrow and a cell showing expression of EYFP-MLN51 and FMRP-positive foci is indicated by an asterisk. (B) Silencing of MLN51 alters SG formation. SGs were traced using an anti-FMRP antibody in arsenite-treated HeLa cells transfected with either synthetic control siRNA (siRNA/control, black bar) or MLN51-specific siRNA (siRNA/MLN51, white bar). The numbers of cells showing clear FMRP-positive foci were counted. Values presented are mean percentages  $\pm$  s.e.m. of  $n=2$  independent experiments done in triplicate, with \*\*\* indicating a  $P$  value of less than 0.001. (C) Depletion of MLN51 results in reduced cell viability following stress. HeLa cells were transfected with either control synthetic siRNA (black circles) or MLN51-specific siRNA (white circles). 48 hours after transfection, cells were stressed with sorbitol for 2.5 hours, followed by incubation in normal medium. Cellular viability was measured at each time point. Values presented are mean percentages  $\pm$  s.e.m. of a typical experiment made in triplicate with \*\* and \*\*\* indicating a  $P$  value of less than 0.01 and 0.001, respectively. Top right: western blot analysis showing the level of MLN51 depletion in the experiment presented.



### MLN51 increases cell viability following stress

Recently, hnRNP A1 was found to participate in the stress response by increasing cell recovery after stress (Guil et al., 2006). We similarly addressed the physiological role of MLN51 in the stress response, using HeLa cells, depleted or not of MLN51 with RNAi. HeLa cells were treated with sorbitol for 2.5 hours, washed and normal medium was added during the recovery period. Cell viability was assayed by measuring the amount of intracellular ATP before, during and after stress. Sorbitol treatment of HeLa cells (for 2.5 hours) induced SG formation, as traced by MLN51 and FMRP (not shown). As shown in Fig. 6C, control siRNA-treated cells recovered well after a few hours. By contrast, MLN51 siRNA-treated cells lost viability during stress and recovered poorly after stress release. Collectively, these results show that MLN51 plays a broad role in the stress response by participating in SG assembly during stress and by favouring cell recovery following stress.

### Breast cancer cells accumulate cytoplasmic foci resembling SGs

We have previously reported that, in breast cancer biopsies, immunolocalization of MLN51 in cancer cells indicates granular distribution (Degot et al., 2002). In breast tumours overexpressing the protein, MLN51 was found to be either

diffuse in the cytoplasm (Fig. 7Aa) or in cytoplasmic granules (Fig. 7Ab). In some samples, both types of localization were evident in discrete regions of the tumour (not shown). Fifteen out of 31 MLN51-positive breast tumours observed showed a partial or complete granular localization of MLN51. Since this localization is reminiscent of SGs, we performed colocalization studies using antibodies raised against proteins normally present in SGs. As shown in Fig. 7B, FMRP and PABP were present in cytoplasmic granules positive for MLN51. Taken together, our data indicate that, in MLN51-positive breast cancer cells, the protein can be found in cytoplasmic structures which are similar to SGs of cultured stressed cells. As FMRP and PABP are present in a variety of mRNA granules, further studies, using more specific SG markers, will be required to better identify the foci observed in breast cancer tissues.

### Discussion

MLN51 is a component of the EJC core, a tetrameric complex formed by the splicing-dependent association of four proteins, MAGOH, Y14, EIF4A3 and MLN51, with mRNA (Ballut et al., 2005; Tange et al., 2005; Stroupe et al., 2006; Andersen et al., 2006; Bono et al., 2006). The EJC is assembled in the nucleus and plays important roles in the post-transcriptional regulation of gene expression including translation and mRNA



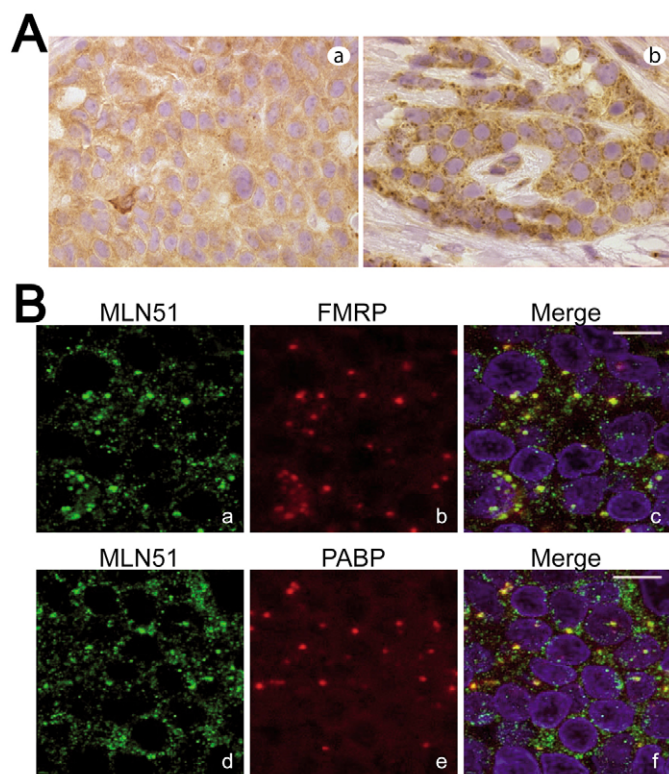


**Fig. 7.** MLN51-overexpressing breast tumours contain cytoplasmic foci resembling SGs. (A) Immunohistochemical analysis of MLN51 subcellular localization in two ductal carcinomas. In cancer cells, MLN51 staining is either diffuse in the cytoplasm (a) or appears in punctate cytoplasmic structures (b). Sections are counterstained with Haematoxylin (nuclei are violet). (B) MLN51-expressing tumours were double-stained for MLN51 (green) and FMRP (red) or with MLN51 (green) and PABP (red). Nuclei were counterstained with Hoechst (blue). Note that both FMRP and PABP are present in cytoplasmic foci positive for MLN51. Bar, 10  $\mu$ m.

turnover (Tange et al., 2004). Among the four EJC core proteins, only MLN51 is predominantly cytoplasmic, and the reason for this localization is unclear. Two non-exclusive hypotheses can be proposed: (1) the cytoplasmic localization of MLN51 has a regulatory function, and its import into the nucleus might be a limiting step in EJC assembly; (2) aside from its role in the EJC, MLN51 participates in other cellular functions in the cytoplasm.

In the present study, we showed that under stress conditions, MLN51 colocalizes with FMRP, TIA1, PABP and poly(A)<sup>+</sup> RNA in SGs, indicating that MLN51 is a novel SG component. SGs are cytoplasmic aggregates composed of proteins and RNAs, formed under unfavourable conditions; they represent an adaptive cellular response to environmental stress, and are mainly known as dynamic cytoplasmic foci where stalled 48S preinitiation complexes accumulate (Kedersha et al., 2002). Many SG-resident proteins are RNA-binding proteins involved in different aspects of mRNA function, such as translation (TIA1, TIAR and PABP), stability (HuR, TTP), degradation (G3BP and PMR1) and localization (Staufen, Smaug and FMRP) (Anderson and Kedersha, 2006). Interestingly, some of

these RNA-binding proteins, such as TIA1 and TIAR, were shown to rapidly shuttle in and out of SGs, supporting the notion that SGs are not static storage centres for untranslated mRNA, but rather, dynamic structures which sort specific mRNA transcripts for reinitiation or decay (Anderson and Kedersha, 2006; Kedersha and Anderson, 2002). Using FRAP, TIA1 was previously shown to rapidly shuttle in and out of SGs (Kedersha et al., 2000). More recently, hnRNPA1 was found to shuttle in and out of SGs as rapidly as TIA1 (Guil et al., 2006). By contrast, the same study showed that PABP moved slowly with a large proportion of the protein being immobile (Guil et al., 2006). Similar to hnRNPA1, the C-terminal half of MLN51 shuttles very rapidly in and out of SGs. Full length MLN51 resides longer in SGs than MLN51Ct and hnRNPA1 but MLN51 is mobile and rapidly exchanged compared with PABP. Our data, together with its homology with the *Drosophila* mRNA transporter Barentsz (van Eeden et al., 2001), its presence in neuronal mRNA transport granules (Macchi et al., 2003) and its mobility within SGs, suggest that MLN51 could be involved in mRNA targeting to SGs. Recently other proteins, not yet related to RNA metabolism, were found in SGs. Indeed, plakophilins 1 and 3, known as architectural components in plaques of desmosomes, are present in SGs, suggesting that proteins acting at cell-cell junctions might influence mRNA metabolism and vice versa (Hofmann et al., 2006).

The C-terminal ~220 amino acid region is responsible for the recruitment of MLN51 into SGs. This region is dispensable for the incorporation of MLN51 into the EJC (Degot et al., 2004). We were unable to narrow down this addressing domain because shorter deletion mutants were mainly retained in the nucleus. Bioinformatic analysis of this region revealed the presence of a variety of potential consensus motifs, including several phosphorylation sites at serine residues, SH2 and SH3 binding sites and a conserved glutamine-rich region (amino acids 608-675) (Degot et al., 2004; Degot et al., 2002). Interestingly, two SG-resident proteins, TIA1 and Pumilio 2, have been shown to be targeted to SGs via a glutamine-rich prion-related domain (PRD) which is responsible for their self-aggregation (Gilks et al., 2004; Vessey et al., 2006). It is therefore possible that the conserved MLN51 glutamine-rich region participates in SG localization. Phosphorylation has been shown to regulate the recruitment of other proteins to SGs: TTP phosphorylation at specific serine residues prevents its recruitment into SGs (Stoecklin et al., 2004), whereas G3BP phosphorylation at serine 149 is required for its association with SGs (Tourriere et al., 2003). MLN51 possesses many potential phosphorylation sites and was found to be phosphorylated in both normal and cancer-derived cells (Degot et al., 2002). Therefore, phosphorylation at specific residues may govern its association with SGs.

Several proteins act to modulate SG formation and the central role of the translation initiation factor EIF2 $\alpha$  is well established (Anderson and Kedersha, 2006). Under conditions where cellular homeostasis is altered, phosphorylation of EIF2 $\alpha$  by stress-activated kinases triggers SG assembly (Kedersha et al., 1999; Kimball et al., 2003). The notion that SGs can assemble in the absence of EIF2 $\alpha$  phosphorylation was recently reported. Indeed, impairing ribosome recruitment by interfering with EIF4A activity induces SGs in the absence of EIF2 $\alpha$  phosphorylation, signifying that SGs assemble when

the translation-initiation is blocked through EIF2 $\alpha$  phosphorylation-dependent and -independent pathways (Mazroui et al., 2006). Some proteins involved in distinct aspects of mRNA metabolism have been found to induce SG formation (Anderson and Kedersha, 2006). The dominant action on SG assembly by TIA1, TIAR and G3BP is self-aggregation (Gilks et al., 2004; Tourriere et al., 2003). Similarly, proteins acting on translational repression, such as FMRP, Smaug, Pumilio 2 and CPEB, can induce SG formation in the absence of stress (Baez and Boccaccio, 2005; Mazroui et al., 2002; Vessey et al., 2006; Wilczynska et al., 2005). FMRP induces SGs via a specific RGG box (Mazroui et al., 2002), a protein domain involved in RNA recognition and binding to G-quartet motifs present on cellular mRNAs (Darnell et al., 2001; Schaeffer et al., 2001). The translational repressor protein Smaug was recently implicated in SG-related foci formation (Baez and Boccaccio, 2005), and the translation inhibitor, CPEB was also found to dominantly induce SG formation (Wilczynska et al., 2005). Interestingly, the neuronal translation inhibitor Pumilio 2 is also involved in SG formation. Its overexpression in neurons induces SGs, and conversely, its downregulation slightly reduces the capacity to form SGs (Vessey et al., 2006). Since all of these factors act to prevent translation, their overexpression may disrupt posttranslational mRNA metabolism and favour mRNA remobilization into SGs (Baez and Boccaccio, 2005; Mazroui et al., 2002; Vessey et al., 2006; Wilczynska et al., 2005). In striking contrast, MLN51 overexpression does not promote SG formation, and MLN51 is a positive effector of mRNA translation (Tange et al., 2005). Remarkably, MLN51 downregulation, by silencing or by overexpressing a mutant lacking its C-terminal half, prevents SG assembly. This effect appears to be independent of EIF2 $\alpha$  phosphorylation.

MLN51 plays a physiological role in the stress response since its depletion significantly reduces cell recovery following stress. Similarly, hnRNPA1, a nucleocytoplasmic shuttling protein involved in many aspects of mRNA metabolism, also supports cell viability following stress (Guil et al., 2006). Moreover, hnRNPA1 is associated with apoptosis resistance (Patry et al., 2003) and increased proliferation (He et al., 2005) in cancer cells, two important features of cancer cells. A functional link between SGs and cell death via tumour necrosis factor (TNF) signalling has been established recently (Kim et al., 2005). TNF receptor associated factor 2 (TRAF2), a central mediator of NF $\kappa$ B activation (Chung et al., 2002), is trapped into SGs, and its sequestration prevents TNF-induced apoptosis under stress conditions (Kim et al., 2005). A connection between SGs and tumour radioresistance was also established previously in mice (Ruas and Poellinger, 2005). Hypoxia-inducible factor-1 (HIF-1) is a transcription factor activated by hypoxia that modulates a variety of genes involved in many biological processes, including angiogenesis (Semenza, 2003). HIF-1 proangiogenic activity increases in tumours following radiation; this action is due, in part, to the sequestration of HIF-1 target gene mRNAs in SGs in hypoxic tumours (Ruas and Poellinger, 2005). Sequestration is relieved when SGs are dissociated following radiation therapy and subsequent reoxygenation, which results in the translation of HIF-1 dependent transcripts and promote tumour progression (Ruas and Poellinger, 2005; Moeller and Dewhirst, 2006). Importantly, in some human breast tumours overexpressing

MLN51, we showed that the protein localizes with FMRP and PABP in cytoplasmic foci resembling SGs. However, further studies will be necessary to formally identify these foci as SGs. Altogether these data support the concept that SGs exist in tumours where they may support cancer cell survival in unfavourable conditions such as hypoxia and/or cell death induced by cytokines.

MLN51 has distinct functions in mRNA metabolism as an EJC and SG component. In this study, we provide evidence that MLN51 acts in SG modelling independent of its association with the EJC, and that SG-related structures exist in breast tumour cells. Future studies will be necessary to define the specific function of MLN51 in SGs and how the presence of SG-related structures influences cancer cell behaviour.

## Materials and Methods

### Antibodies

MLN51 was detected using a monoclonal antibody (anti-SELOR) obtained by immunization with the recombinant protein corresponding to the SELOR domain (residues 137-283) or using polyclonal antibodies recognizing the SELOR domain, the C- or the N-terminal part of MLN51 (Degot et al., 2002; Degot et al., 2004). The rabbit anti-FMRP and anti-DCP1A antibodies were a kind gift from B. Bardoni (IGBMC, Illkirch, France) and B. Séraphin (CGM, Gif-sur-Yvette, France), respectively. Goat anti-TIA1, rabbit anti-EIF2 $\alpha$ , rabbit anti-phospho-EIF2 $\alpha$  and mouse anti-Flag were from Santa Cruz Biotechnology, Cell Signaling Technology or Sigma. The monoclonal anti-PABP and anti-tubulin were from Santa Cruz Biotechnology. Cy3-conjugated affinity-purified donkey anti-mouse, anti-rabbit and anti-goat IgG and Cy5-conjugated affinity-purified donkey anti-goat IgG were purchased from Interchim (Montluçon, France) and Alexa Fluor 488-conjugated donkey anti-rabbit and anti-mouse IgG from Molecular Probes (Eugene, OR, USA).

### Plasmids construction and transfection

The vectors encoding MLN51 and truncated versions of the protein fused to the enhanced yellow fluorescent protein (EYFP) and the Flag-MLN51Nt fusion proteins were previously described (Degot et al., 2004; Degot et al., 2002). The complete open reading frames of MAGOH (accession no. NM\_002370) and Y14/RNA binding motif protein 8 (RBM8) (accession no. NM\_005105) were obtained by RT-PCR using Flag-tagged constructs (Degot et al., 2004) and the following synthetic oligonucleotides: 5' primer (ACAATTGTGG GAGCCATGGA GAGTGACTTT), 3' primer (GACAATTGGG ATTGGTTTAA TCTTGAAGTG) and 5' primer (GACAATTGTG CGGACGTGCT AGATCTTCAC), 3' primer (GACAATTGTC TGTCAGCGAC GTCTCCGGTC) and inserted into the pSTBLUE1 vector (Novagen, Darmstadt, Germany). The inserts were released by *MunI* digestion and inserted in frame into the *EcoRI* site of the pEYFP-C1 expression vector (Clontech), thus generating pEYFP-MAGOH and pEYFP-Y14 plasmids. The siRNA-insensible EYFP-MLN51 plasmid (pEYFP-MLN51ins) was obtained from pEYFP-MLN51 vector by site-directed mutagenesis (primer: TGATGATGAAG ATCGTAAAAAT CCAGCATAACATA) which replaces two guanines with thymine and adenine but respects the coding sequence. The expression of this modified protein is not affected by the silencing using MLN51 siRNA as verified by immunohistochemistry and western blot analysis.

For stable transfection, PCR fragments corresponding to MLN51/1-703 or MLN51/1-383 were released using *MunI* digestion from their pSTBLUE1 intermediate vector (Degot et al., 2004); and inserted into the *EcoRI* site of pUHD10.3 plasmid (Gossen et al., 1995) thus generating pUHD-MLN51/1-703 and pUHD-MLN51/1-383.

The vector encoding DCP1 protein fused to the enhanced green fluorescent protein (EGFP) was a kind gift from Bertrand Séraphin. The vectors encoding GFP-hnRNPA1 and GFP-PABP were a gift from Javier F. Cáceres (MRC Edinburgh, UK).

### Cell cultures and transfection

HeLa cells were maintained in DMEM supplemented with 5% foetal calf serum. For transient transfection in 24-well plates, 1  $\mu$ g of vector was transfected using Jet Pei (Polyplus transfection, Illkirch, France). For stress induction, cells were treated with 0.5 mM arsenite or 1  $\mu$ M of hippuristanol for 30 minutes.

For stable transfection using the Tet-On inducible gene expression system, HeLa Tet-On cells were purchased (Clontech, Mountain View, CA, USA), maintained and transfected with plasmids allowing the inducible expression of MLN51Fl or MLN51Nt. Stable cell lines were obtained by co-transfection of 9  $\mu$ g pUHD-MLN51/1-703 (Fl) or pUHD-MLN51/1-383 (Nt) plasmids with 1  $\mu$ g of hygromycin-resistant pSV2 plasmid per 100 mm diameter dish using Jet Pei. Stable clones were selected with hygromycin-containing medium. The Tet promoter was

induced by addition of 1 µg/ml doxycyclin to the culture medium for 24 hours. The HeLa Tet-On cells were then treated with 0.5 mM arsenite or 1 µM hippuristanol for 30 minutes. Hippuristanol was a kind gift from Junichi Tanaka (University of the Ryukyus, Nishihara, Okinawa, Japan).

### siRNA transfection

Silencing using synthetic siRNA was used to decrease the level of MLN51 in HeLa cells. Control and MLN51 siRNAs were obtained from Eurogentec (Liège, Belgium) (MLN51 target sequence: 5'-GATCGGAAGAATCCAGCAT-3'). HeLa cells were transfected twice (24-hour interval) with control or MLN51 siRNAs using Lipofectamine Plus Reagent (Invitrogen) as directed by the manufacturer.

### Immunofluorescence

HeLa cells were seeded on glass coverslips in 24-well plates. After 24-72 hours in culture, cells were washed with PBS, fixed for 5 minutes at room temperature in 4% paraformaldehyde in PBS and permeabilized for 10 minutes with 0.1% Triton X-100 in PBS. After blocking in 1% bovine serum albumin in PBS, cells were incubated at room temperature with the primary antibodies for 1 hour. Cells were washed three times in PBS and incubated for 30 minutes with Cy3 or Alexa Fluor 488-conjugated appropriate secondary antibody (1:500) for 30 minutes. Cells were washed three times in PBS and nuclei were counterstained with Hoechst-33258 dye. Slides were mounted in Vectashield (Polysciences Inc., Warrington, PA, USA). Observations were made with a fluorescence microscope (Leica DMLB 30T, Leica Microsystems, Wetzlar Germany) or with confocal microscopes (Leica SP1 and Leica SP2-MP, Leica Microsystems).

### Fluorescence in situ hybridization

HeLa cells grown on coverslips, were washed with PBS, fixed for 5 minutes at room temperature in 4% paraformaldehyde in PBS and permeabilized for 10 minutes with 0.1% Triton X-100 in PBS. Cells were incubated in 2× SSC-50% formamide for 5 minutes and hybridized overnight at 37°C with hybridization buffer (20 ng/ml oligo(dT) probe fluorescently labelled with Cy3, 2× SSC, 50% formamide, 30 µg/ml *E. coli* tRNA, 0.02% RNase-free BSA, 2 mM vanadyl-ribonucleoside complex, 1% dextran sulfate). The oligo(dT) probe (40 Ts) was fluorescently labelled with Cy3. Cells were washed three times for 30 minutes at 37°C in 2× SSC-50% formamide. Immunofluorescence microscopy was performed as described above.

### Immunohistochemistry and immunohistofluorescence

Immunohistochemical and immunohistofluorescence analysis was performed on paraffin-embedded tissue sections of human breast carcinoma samples as described previously (Degot et al., 2002). For immunohistochemical analysis, tissue sections were incubated with anti-MLN51Ct polyclonal antibody and a peroxidase-anti-peroxidase system (Dako, Carpinteria, CA, USA) was used for its identification. For immunohistofluorescence, the rabbit anti-MLN51Ct, mouse anti-PABP and mouse anti-FMRP antibodies were used and microscopy was performed as described above.

### Western blotting

HeLa cells were collected and washed in 1× PBS. Lysis was performed by incubating the cells 30 minutes at 4°C in 150 µl of lysis buffer (50 mM Tris-HCl pH 7.5, 150 mM NaCl, 1 mM EDTA, 1% Triton X-100, 1× protease inhibitor cocktail). Soluble proteins were recovered after centrifugation at 10,000 g at 4°C for 10 minutes and quantified by the Bradford method (Bio-Rad). 20 µg of proteins were mixed with SDS sample buffer (50 mM Tris-HCl pH 6.8, 2% SDS, 10% glycerol, 1.4 M β-mercaptoethanol, Bromophenol Blue), separated using SDS-8.5% polyacrylamide gel electrophoresis, and electrotransferred to nitrocellulose sheets (Schleicher and Schuell, Dassel, Germany). The membrane was blocked in PBS containing 3% nonfat dry milk and 0.1% Tween 20. Rabbit anti-MLN51Ct, anti-EIF2a and anti-phospho-EIF2a were used as primary antibodies at dilution of 1:1000 and monoclonal anti-tubulin was used at dilution of 1:10,000. After washing, the blots were incubated with appropriate secondary antibodies. Horseradish peroxidase-conjugated (HRP) AffiniPure donkey anti-rabbit or goat anti-mouse at 1:10000 (Jackson ImmunoResearch) and HRP donkey anti-goat at 1:1000 (Santa Cruz Biotechnology) were used. Finally, protein-antibody complexes were visualized by an enhanced chemiluminescence detection system (ECL detection reagent, Amersham).

### Fluorescence recovery after photobleaching (FRAP)

HeLa cells were plated on glass-bottomed dishes and incubated in a microscopic chamber (at 37°C), mounted on an inverted Nikon TE2000 microscope. Z-stacks were collected every 3 seconds, on a CCD camera (Cascade 512K, Roper Scientific), and the bleach was done with a 488 laser controlled by a confocal head (Nikon). Z-stacks were then averaged and the fluorescence intensity in the bleach zone was measured in the time series.

### Cell viability assay

HeLa cells were plated on 96-well plates and transfected twice with control or

MLN51 siRNAs. At 48 hours after the second transfection, cells were stressed with 0.6 M sorbitol for 2.5 hours, washed and incubated in normal medium. Cell viability was monitored during and after stress release using CellTiterGlo (Promega) as directed by the manufacturer. The luminescence, corresponding to the viable cell number, was read with a Centro XS<sup>3</sup> LB 960 (Berthold Technologies). Three independent experiments were performed in triplicate, and the results of the most representative experiment are shown.

The authors thank S. Chan and F. Alpy for critical reading of the manuscript, M. Gintz for technical assistance, the IGBMC mouse monoclonal and rabbit polyclonal facilities, the IGBMC cell culture facility and the IGBMC Imaging Centre Technology Platform. A.B. and S.D. were recipients of a French Ministère de la Recherche et de la Technologie (MRT) and of a Ligue Nationale Française Contre le Cancer (LNCC) comité du Haut-Rhin fellowships, respectively. N.C. is a recipient of an Association pour la Recherche sur le Cancer (ARC) fellowship. This work was supported by an Association pour la Recherche sur le Cancer (ARC) grant (project N°: 3867) to C.T., by a grant from the French National Agency for Research (ANR) (# ANR-05-BLAN-0118) to H.L.H., E.B. and C.T., and by funds from the Institut National de la Santé et de la Recherche Médicale (INSERM), Centre National de la Recherche Scientifique (CNRS) and the Université Louis Pasteur (ULP).

### References

- Andersen, C. B., Ballut, L., Johansen, J. S., Chamieh, H., Nielsen, K. H., Oliveira, C. L., Pedersen, J. S., Seraphin, B., Le Hir, H. and Andersen, G. R. (2006). Structure of the exon junction core complex with a trapped DEAD-box ATPase bound to RNA. *Science* **313**, 1968-1972.
- Anderson, P. and Kedersha, N. (2006). RNA granules. *J. Cell Biol.* **172**, 803-808.
- Baez, M. V. and Boccaccio, G. L. (2005). Mammalian Smaug is a translational repressor that forms cytoplasmic foci similar to stress granules. *J. Biol. Chem.* **280**, 43131-43140.
- Ballut, L., Marchadier, B., Bague, A., Tomasetto, C., Seraphin, B. and Le Hir, H. (2005). The exon junction core complex is locked onto RNA by inhibition of eIF4AIII ATPase activity. *Nat. Struct. Mol. Biol.* **12**, 861-869.
- Bono, F., Ebert, J., Lorentzen, E. and Conti, E. (2006). The crystal structure of the exon junction complex reveals how it maintains a stable grip on mRNA. *Cell* **126**, 713-725.
- Bordeleau, M. E., Mori, A., Oberer, M., Lindqvist, L., Chard, L. S., Higa, T., Belsham, G. J., Wagner, G., Tanaka, J. and Pelletier, J. (2006). Functional characterization of IRESes by an inhibitor of the RNA helicase eIF4A. *Nat. Chem. Biol.* **2**, 213-220.
- Chung, J. Y., Park, Y. C., Ye, H. and Wu, H. (2002). All TRAFs are not created equal: common and distinct molecular mechanisms of TRAF-mediated signal transduction. *J. Cell Sci.* **115**, 679-688.
- Cougot, N., Babajko, S. and Seraphin, B. (2004). Cytoplasmic foci are sites of mRNA decay in human cells. *J. Cell Biol.* **165**, 31-40.
- Custodio, N., Carvalho, C., Condado, I., Antoniou, M., Blencowe, B. J. and Carmo-Fonseca, M. (2004). In vivo recruitment of exon junction complex proteins to transcription sites in mammalian cell nuclei. *RNA* **10**, 622-633.
- Darnell, J. C., Jensen, K. B., Jin, P., Brown, V., Warren, S. T. and Darnell, R. B. (2001). Fragile X mental retardation protein targets G quartet mRNAs important for neuronal function. *Cell* **107**, 489-499.
- Degot, S., Regnier, C. H., Wendling, C., Chenard, M. P., Rio, M. C. and Tomasetto, C. (2002). Metastatic Lymph Node 51, a novel nucleo-cytoplasmic protein overexpressed in breast cancer. *Oncogene* **21**, 4422-4434.
- Degot, S., Le Hir, H., Alpy, F., Kedinger, V., Stoll, L., Wendling, C., Seraphin, B., Rio, M. C. and Tomasetto, C. (2004). Association of the breast cancer protein MLN51 with the exon junction complex via its speckle localizer and RNA binding module. *J. Biol. Chem.* **279**, 33702-33715.
- Eulalio, A., Behm-Ansmant, I. and Izaurralde, E. (2007). P bodies: at the crossroads of post-transcriptional pathways. *Nat. Rev. Mol. Cell Biol.* **8**, 9-22.
- Gehring, N. H., Kunz, J. B., Neu-Yilik, G., Breit, S., Viegas, M. H., Hentze, M. W. and Kulozik, A. E. (2005). Exon-junction complex components specify distinct routes of nonsense-mediated mRNA decay with differential cofactor requirements. *Mol. Cell* **20**, 65-75.
- Gilks, N., Kedersha, N., Ayodele, M., Shen, L., Stoecklin, G., Dember, L. M. and Anderson, P. (2004). Stress granule assembly is mediated by prion-like aggregation of TIA-1. *Mol. Biol. Cell* **15**, 5383-5398.
- Gossen, M., Freundlieb, S., Bender, G., Muller, G., Hillen, W. and Bujard, H. (1995). Transcriptional activation by tetracyclines in mammalian cells. *Science* **268**, 1766-1769.
- Guil, S., Long, J. C. and Caceres, J. F. (2006). hnRNP A1 relocalization to the stress granules reflects a role in the stress response. *Mol. Cell Biol.* **26**, 5744-5758.
- He, Y., Brown, M. A., Rothnagel, J. A., Saunders, N. A. and Smith, R. (2005). Roles of heterogeneous nuclear ribonucleoproteins A and B in cell proliferation. *J. Cell Sci.* **118**, 3173-3183.
- Hofmann, I., Casella, M., Schnolzer, M., Schlechter, T., Spring, H. and Franke, W.

- W. (2006). Identification of the junctional plaque protein plakophilin 3 in cytoplasmic particles containing RNA-binding proteins and the recruitment of plakophilins 1 and 3 to stress granules. *Mol. Biol. Cell* **17**, 1388-1398.
- Ivanov, P. A., Chudinova, E. M. and Nadezhkina, E. S. (2003). Disruption of microtubules inhibits cytoplasmic ribonucleoprotein stress granule formation. *Exp. Cell Res.* **290**, 227-233.
- Kataoka, N., Yong, J., Kim, V. N., Velazquez, F., Perkinson, R. A., Wang, F. and Dreyfuss, G. (2000). Pre-mRNA splicing imprints mRNA in the nucleus with a novel RNA-binding protein that persists in the cytoplasm. *Mol. Cell* **6**, 673-682.
- Kedersha, N. and Anderson, P. (2002). Stress granules: sites of mRNA triage that regulate mRNA stability and translatability. *Biochem. Soc. Trans.* **30**, 963-969.
- Kedersha, N. L., Gupta, M., Li, W., Miller, I. and Anderson, P. (1999). RNA-binding proteins TIA-1 and TIAR link the phosphorylation of eIF-2 alpha to the assembly of mammalian stress granules. *J. Cell Biol.* **147**, 1431-1442.
- Kedersha, N., Cho, M. R., Li, W., Yacono, P. W., Chen, S., Gilks, N., Golan, D. E. and Anderson, P. (2000). Dynamic shuttling of TIA-1 accompanies the recruitment of mRNA to mammalian stress granules. *J. Cell Biol.* **151**, 1257-1268.
- Kedersha, N., Chen, S., Gilks, N., Li, W., Miller, I. J., Stahl, J. and Anderson, P. (2002). Evidence that ternary complex (eIF2-GTP-tRNA(i)(Met))-deficient preinitiation complexes are core constituents of mammalian stress granules. *Mol. Biol. Cell* **13**, 195-210.
- Kim, W. J., Back, S. H., Kim, V., Ryu, I. and Jang, S. K. (2005). Sequestration of TRAF2 into stress granules interrupts tumour necrosis factor signaling under stress conditions. *Mol. Cell Biol.* **25**, 2450-2462.
- Kimball, S. R., Horetsky, R. L., Ron, D., Jefferson, L. S. and Harding, H. P. (2003). Mammalian stress granules represent sites of accumulation of stalled translation initiation complexes. *Am. J. Physiol. Cell Physiol.* **284**, C273-C284.
- Le Hir, H., Izaurralde, E., Maquat, L. E. and Moore, M. J. (2000). The spliceosome deposits multiple proteins 20-24 nucleotides upstream of mRNA exon-exon junctions. *EMBO J.* **19**, 6860-6869.
- Le Hir, H., Gatfield, D., Braun, I. C., Forler, D. and Izaurralde, E. (2001). The protein Mago provides a link between splicing and mRNA localization. *EMBO Rep.* **2**, 1119-1124.
- Liu, J., Valencia-Sanchez, M. A., Hannon, G. J. and Parker, R. (2005). MicroRNA-dependent localization of targeted mRNAs to mammalian P-bodies. *Nat. Cell Biol.* **7**, 719-723.
- Macchi, P., Kroening, S., Palacios, I. M., Baldassa, S., Grunewald, B., Ambrosino, C., Goetze, B., Lupas, A., St Johnston, D. and Kiebler, M. (2003). Barentsz, a new component of the Staufen-containing ribonucleoprotein particles in mammalian cells, interacts with Staufen in an RNA-dependent manner. *J. Neurosci.* **23**, 5778-5788.
- Marciniak, S. J., Garcia-Bonilla, L., Hu, J., Harding, H. P. and Ron, D. (2006). Activation-dependent substrate recruitment by the eukaryotic translation initiation factor 2 kinase PERK. *J. Cell Biol.* **172**, 201-209.
- Mazroui, R., Huot, M. E., Tremblay, S., Filion, C., Labelle, Y. and Khandjian, E. W. (2002). Trapping of messenger RNA by Fragile X Mental Retardation protein into cytoplasmic granules induces translation repression. *Hum. Mol. Genet.* **11**, 3007-3017.
- Mazroui, R., Sukarieh, R., Bordeleau, M. E., Kaufman, R. J., Northcote, P., Tanaka, J., Gallouzi, I. and Pelletier, J. (2006). Inhibition of ribosome recruitment induces stress granule formation independently of eukaryotic initiation factor 2alpha phosphorylation. *Mol. Biol. Cell* **17**, 4212-4219.
- Moeller, B. J. and Dewhirst, M. W. (2006). HIF-1 and tumour radiosensitivity. *Br. J. Cancer* **95**, 1-5.
- Nott, A., Le Hir, H. and Moore, M. J. (2004). Splicing enhances translation in mammalian cells: an additional function of the exon junction complex. *Genes Dev.* **18**, 210-222.
- Palacios, I. M., Gatfield, D., St Johnston, D. and Izaurralde, E. (2004). An eIF4AIII-containing complex required for mRNA localization and nonsense-mediated mRNA decay. *Nature* **427**, 753-757.
- Parker, R. and Sheth, U. (2007). P bodies and the control of mRNA translation and degradation. *Mol. Cell* **25**, 635-646.
- Patry, C., Bouchard, L., Labrecque, P., Gendron, D., Lemieux, B., Toutant, J., Lapointe, E., Wellinger, R. and Chabot, B. (2003). Small interfering RNA-mediated reduction in heterogeneous nuclear ribonucleoproteins A1/A2 proteins induces apoptosis in human cancer cells but not in normal mortal cell lines. *Cancer Res.* **63**, 7679-7688.
- Pillai, R. S., Bhattacharyya, S. N., Artus, C. G., Zoller, T., Cougot, N., Basyuk, E., Bertrand, E. and Filipowicz, W. (2005). Inhibition of translational initiation by Let-7 MicroRNA in human cells. *Science* **309**, 1573-1576.
- Ruas, J. L. and Poellinger, L. (2005). Hypoxia-dependent activation of HIF into a transcriptional regulator. *Semin. Cell Dev. Biol.* **16**, 514-522.
- Schaeffer, C., Bardoni, B., Mandel, J. L., Ehresmann, B., Ehresmann, C. and Moine, H. (2001). The fragile X mental retardation protein binds specifically to its mRNA via a purine quartet motif. *EMBO J.* **20**, 4803-4813.
- Semenza, G. L. (2003). Targeting HIF-1 for cancer therapy. *Nat. Rev. Cancer* **3**, 721-732.
- Shibuya, T., Tange, T. O., Sonenberg, N. and Moore, M. J. (2004). eIF4AIII binds spliced mRNA in the exon junction complex and is essential for nonsense-mediated decay. *Nat. Struct. Mol. Biol.* **11**, 346-351.
- Stoecklin, G., Stubbs, T., Kedersha, N., Wax, S., Rigby, W. F., Blackwell, T. K. and Anderson, P. (2004). MK2-induced tristetraprolin:14-3-3 complexes prevent stress granule association and ARE-mRNA decay. *EMBO J.* **23**, 1313-1324.
- Stroupe, M. E., Tange, T. O., Thomas, D. R., Moore, M. J. and Grigorieff, N. (2006). The three-dimensional architecture of the EJC core. *J. Mol. Biol.* **360**, 743-749.
- Tange, T. O., Nott, A. and Moore, M. J. (2004). The ever-increasing complexities of the exon junction complex. *Curr. Opin. Cell Biol.* **16**, 279-284.
- Tange, T. O., Shibuya, T., Jurica, M. S. and Moore, M. J. (2005). Biochemical analysis of the EJC reveals two new factors and a stable tetrameric protein core. *RNA* **11**, 1869-1883.
- Tomasetto, C., Regnier, C., Moog-Lutz, C., Mattei, M. G., Chenard, M. P., Lidereau, R., Basset, P. and Rio, M. C. (1995). Identification of four novel human genes amplified and overexpressed in breast carcinoma and localized to the q11-q21.3 region of chromosome 17. *Genomics* **28**, 367-376.
- Tourriere, H., Chebli, K., Zekri, L., Courselaud, B., Blanchard, J. M., Bertrand, E. and Tazi, J. (2003). The RasGAP-associated endoribonuclease G3BP assembles stress granules. *J. Cell Biol.* **160**, 823-831.
- van Eeden, F. J., Palacios, I. M., Petronczki, M., Weston, M. J. and St Johnston, D. (2001). Barentsz is essential for the posterior localization of oskar mRNA and colocalizes with it to the posterior pole. *J. Cell Biol.* **154**, 511-523.
- Vessey, J. P., Vaccani, A., Xie, Y., Dahm, R., Karra, D., Kiebler, M. A. and Macchi, P. (2006). Dendritic localization of the translational repressor Pumilio 2 and its contribution to dendritic stress granules. *J. Neurosci.* **26**, 6496-6508.
- Wilczynska, A., Aigueperse, C., Kress, M., Dautry, F. and Weil, D. (2005). The translational regulator CPEB1 provides a link between dcp1 bodies and stress granules. *J. Cell Sci.* **118**, 981-992.
- Wilhelm, J. E., Hilton, M., Amos, Q. and Henzel, W. J. (2003). Cup is an eIF4E binding protein required for both the translational repression of oskar and the recruitment of Barentsz. *J. Cell Biol.* **163**, 1197-1204.
- Zhang, K. and Kaufman, R. J. (2006). The unfolded protein response: a stress signaling pathway critical for health and disease. *Neurology* **66**, S102-S109.